Sofia University "St. Kliment Ohridski"

Faculty of Physics

Department "Meteorology and Geophysics"

Integrated Water Vapour comparison from GNSS and WRF model for Bulgaria in 2013

Master Thesis

of

Evgenia Stefanova Egova

No 180084

Supervisor:

/Assoc. Prof. G. Guerova/

Head of Department:

/Assoc. Prof. N. Rachev/

Sofia April 2015

Contents

List of Figures

Abstract

Estimates of integrated water vapour derived from the Global Navigational Satellite System (GNSS) and Weather and Research Forecast model (WRF) are compared in this work. The objective of the study is to validate the water vapour field of one operational Numerical Weather Prediction (NWP) WRF model against GNSS-observed IWV and to draw conclusions about future assimilation of IWV. For the study we use the GNSS data processed in collaboration with University of Luxembourg for 2013.

The comparison with the IWV derived from GNSS is made for 7 stations and the closest NWP model grid points. The GNSS provides high temporal resolution of 5 minutes but in this thesis 1 hour resolution is used. To derive IWV from GNSS tropospheric products the surface pressure and temperature are taken from the WRF model. This allows to increase by factor of 3 the temporal resolution of GNSS-IWV. It is to be noted that surface observations in Bulgaria are with temporal resolution 3 hours.

Based on the good agreement between the WRF model surface pressure values with the observed in this work we use the model to derive the GNSS water vapour. The comparison for surface temperature and pressure derived by the Model and by the Observation show good agreement and correlation coefficient over 0.989. This way a higher temporal resolution is achieved. In this work one-hourly data sets are compared. For 5 stations (Burgas, Montana, Lovech, Stara Zagora and Shumen) the diurnal mean comparison between the GNSS-IWV and the WRF model in 2013 show that the IWV is well described with largest differences up to 1.2 mm. The monthly mean comparison show that during the summer months the correlation between GNSS and WRF IWV is 0.8-0.85, while during the winter months it is over 0.9. The annual compar-

ison showed mean difference between GNSS and WRF IWV of the data sets between 0.5 and 1.7 mm. The seasonal variation of the IWV can be seen well with maximum values in June and July. Between April and May the water vapour at stations Rozhen and Varna shows changes, which are likely related to the set-up of the stations.

Chapter 1

Introduction

The atmospheric water vapour is a key element of the hydrologic cycle and participates in precipitation formation, energy transfer and atmospheric stability. Water vapour has relatively short lifetime in the atmosphere, from one week to ten days and its complex life cycle includes vertical and horizontal transport, mixing, condensation, precipitation and evaporation. The water vapour distribution is linked to atmospheric dynamics and is of essential importance for operational weather prediction. Due to its high temporal and spatial variability atmospheric water vapour is very demanding to observe. In the last 20 years new technique called GPS (Global Positioning System, developed by USA) meteorology and then renamed GNSS meteorology, with availability of the other constellations like GLONAS (*http://www.glonass.it/eng/*) system and Galileo (*http://www.gsa.europa.eu/galileo/services*), is used for remote sensing of atmospheric water vapour.

The first major project on GPS meteorology is the COST Action 716 (1999-2004, *http://www.www.oso.chalmers.se/users/kge/cost716.html/*) with participation of 16 European countries. The aim of COST 716 is exploitation of ground-based GPS for climate and numerical weather prediction applications. During COST 716 a demonstration campaign was initiated and carried on to assess the quality of GPS derived tropospheric products (zenith total delay) delivered in near real time (90 min after the observation). The success of the demonstration campaign was a major driver for the implementation of tropo-

spheric products in operational weather prediction at the National Meteorological Services (NMS) in Europe. The COST 716 was followed in 2005 by the EUMETNET EIG GPS Water Vapour Programme: *http://www.egvap.dmi.dk/*. E-GVAP provides ground based GNSS observations for use in operational meteorology in near real time (NRT), NWP and general weather forecasting. E-GVAP is based on a close collaboration between geodesy and meteorology. There are currently 18 NMS as members of E-GVAP, and they collaborate with 17 GNSS analysis centres (ACs), delivering GNSS tropospheric products for over 2000 stations in Europe. The GNSS stations providing data in NRT (green points) for April 18th, 2015 are presented in figure 1.1. It is to be noted that since 2014 data from South-east Europe and in particular Greece are also available on E-GVAP service but not yet in NRT mode (red points in figure

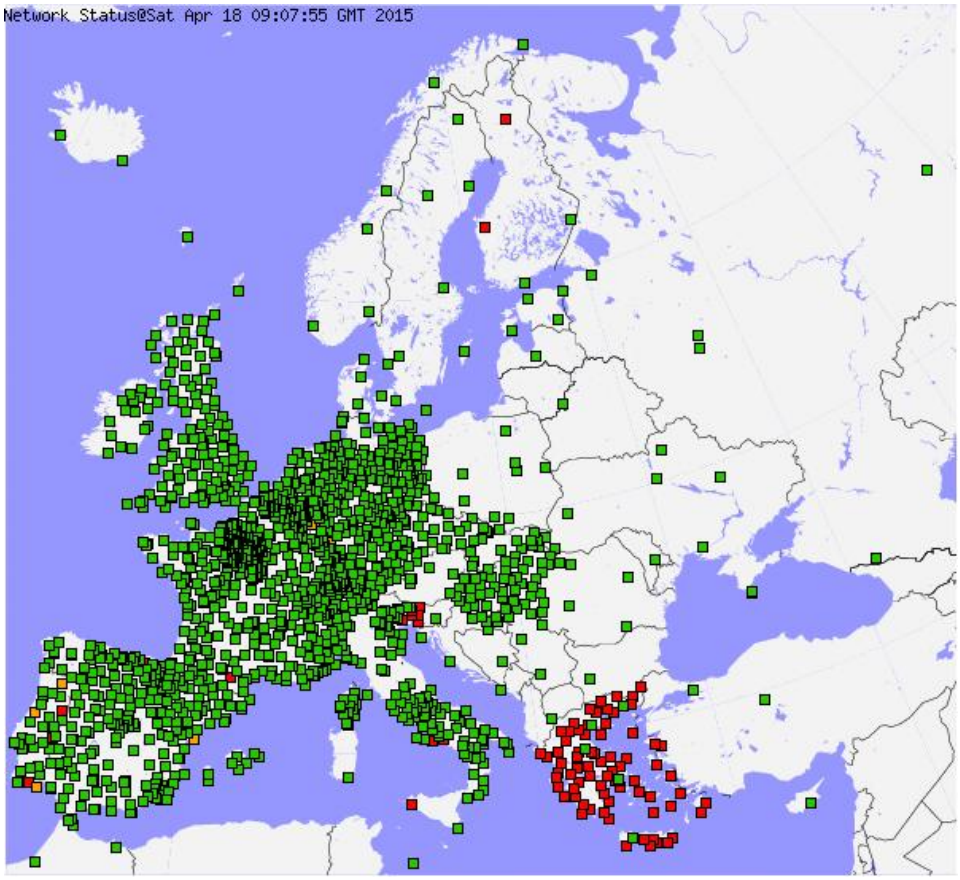

Figure 1.1: GNSS stations delivering tropospheric products for E-GVAP service on 18 April 2015.

1.1). Since 2014 GNSS tropospheric products from 300 sites in North America are included in the E-GVAP service in collaboration with the National Oceanic and Atmospheric Administration (NOAA, *http://www.noaa.gov/*).

NWP models are a major component of the state-of-the-art operational weather forecast. They can be divided into two basic categories: global and local/mesoscale models. The global models are: 1) USA's GFS model (Global Forecast System); 2) the Canadian GEM (Global Environmental Multiscale Model); 3) the IFS (Integrated Forecast System) developed by the European Centre for Medium-Range Weather Forecasts (ECMWF); 4) Unified Model (UM) developed by the UK Met Office; 5) GME developed by the German Weather Service (DWD); 6) ARPEGE developed by Météo-France; 7) Global Spectral Model (GSM) of the Japan Meteorological Agency; 8) GRAPES (Global and Regional Assimilation and PrEdiction System) developed by the China Meteorological Administration; 9) KIAPS-Global Model developed by the Korea Institute of Atmospheric Prediction Systems.

The local mesoscale models used in Europe are developed within four consortium including different NMS. The state-of-the-art model set up of NMS is available via C-SRNWP project (Coordination on Short-Range Numerical Weather Prediction Programme, *http://srnwp.met.hu*). The four consortium are: 1) ALADIN, is high-resolution limited-area hydrostatic and non-hydrostatic model developed by Météo-France and operated by several European and North African countries, including the National Institute for Meteorology and Hydrology in Bulgaria; 2) the COSMO Model, formerly known as LM, aLMo or LAMI, is a limited-area non-hydrostatic model developed within the framework of the Consortium for Small-Scale Modelling (Germany, Switzerland, Italy, Greece, Poland, Romania, and Russia); 3) HIRLAM (High Resolution Limited Area Model), is a cooperation of 9 NMS in Europe; 4) the mesoscale version of the Unified Model operated by the Met Office. On figure (1.2) the operational set-up of the HIRLAM model is presented.

As seen from figure 1.2 WRF model is run as operational NWP model by the NMS in South-east Europe (Bosnia-Herzegovina, Cyprus, Montenegro and Serbia). The WRF model set-up is with horizontal resolution from 2 km to 30 km and vertical resolution up to 64 levels. The forecast range is from $+48h$ to $+216h$ and the boundary conditions are from various global models.

The used in this study WRF set-up is comparable with the state-of-the-art mesoscale models used in the region.

Country	Model		Mesh size (km)	Number of gridpoints	Number of levels	Initial times & Forecast ranges (h)		Type of data assimilation	Model providing LBC data	LBC update interval (h)	Computer
Denmark	HIRLAM	T15	16	610 × 568	40	00/06/12/18	+60h	3D-VAR	ECMWF/IFS	3h	Cray XT5
		K05	5.5	874 × 534	40	00/06/12/18	+48h	3D-VAR	ECMWF/IFS	3h	
		SKA	3.3	874 × 658	65	00/06/12/18	+54h	3D-VAR	ECMWF/IFS	3h	
	HARMONIE	DKA	2.5	800 × 600	65	00/06/12/18	+36h	Surf-ana only	ECMWF/IFS	3h	
		GLA	2.0	200 × 400	65	00/06/12/18	+36h	Surf-ana only	ECMWF/IFS	3h	
Estonia	HIRLAM	ETA II	11	366 × 280	60	00/06/12/18	+54h	3D-VAR fgat	ECMWF/IFS	3h	Linux Cluster
		ETB II	3.3	306 × 306	60	00/12	+36h	3D-VAR fgat	ETA II	1h	
Finland	HIRLAM		7.5	1030 × 816	65	00/06/12/18	+54h	4D-VAR	ECMWF/IFS	3h	Cray XC30
	HARMONIE		2.5	720 × 800	65	00/03/06/09/12/15/18/21	+54h	3D-VAR	ECMWF/IFS	3h	
Iceland	HARMONIE		2.5	300 × 240	65	00/06/12/18	+48h	Surf-ana only	ECMWF/IFS	3h	IBM @ ECMWF
Ireland	HIRLAM		11	654 × 424	60	00/06/12/18	+54h	4D-VAR	ECMWF/IFS	3h	SGI Altix ICE X at ICHEC
	HARMONIE		2.5	540 × 500	60	00/06/12/18	+54h	Surf-ana only	ECMWF/IFS	1h	
Netherlands	HIRLAM		11	726 × 550	60	00/06/12/18	+48h	3D-VAR	ECMWF/IFS	3h	BullX B500
			11	306 × 290	40	00/03/06/../18/21	+60h	3D-VAR	ECMWF/IFS	1h	
			11	306 × 290	40	00/03/06/../18/21	+24h	3D-VAR	HIRLAM	3h	
			11	166 × 152	60	00/01/02/../22/23	+9h	3D-VAR	HIRLAM	1h	Blade system
	HARMONIE		2.5	800 × 800	60	00/03/06/../18/21	+48h	3D-VAR	ECMWF/IFS	1h	BullX B500
			2.5	300 × 300	60	00/12 06/18	+24h +6h	3D-VAR	ECMWF/IFS	3h	at ECMWF
Bosnia-Herzegovina	HRM		14	161 × 161	40	00/12	+72h	none	GME	3h	Linux PC
	WRF-NMM	D1	30	74 × 98	35	00	+48h	none	NCEP/GFS(0.5deg)	3h	
		D2	10	40 × 58	35	00	+48h	Nudging	WRF-NMM(D1)	1h	
	WRF-ARW	D1	18	100 × 68	35	00	+72h	none	NCEP/GFS(0.5deg)	3h	
		D2	6	58 × 61	35	00	+72h	Nudging	WRF-ARW(D1)	1h	
Montenegro	ETA		18	121 × 141	45	00/12	+96h	none	NCEP-GFS(0.5 deg)	3h	Linux Cluster (Intel-Xeon)
	WRF-NMM		7	141 × 202	38	00/12	+96h	none	ECMWF/IFS	3h	
			7	142 × 202	38	00/12	+96h	none	ETA	3h	
			4	58 × 100	38	00/12	+144h	none	ECMWF/IFS	3h	Linux PC
			9	100 × 150	38	00/06/12/18	+120h	none	GFS	3h	
Serbia	ETA		26	145 × 241	32	00/12	+120h	none	GME	6h	Linux PC
	WRF-NMM		4	220 × 290	45	00/12	+72h	none	ECMWF/IFS	3h	HP XC 256 Xeon
			12	260 × 500	38	00/12	+120h	none	GME	3h	HP XC 128 Xeon
			12	260 × 500	38	00/12	+120h	none	GFS	3h	
	NMMB		30	global	64	00	+216h	none	none (global)	-	HP Proliant DL380 G7, 384 Intel Xeon
			10	394 × 326	64	00	+120h	none	NMMB global	3h	
Cyprus	WRF-ARW		2	88 × 55	37	00/12	+120h	none	NCEP/GFS	3h	IBM iDataPlex dx360 M3 (Cyprus Institute Cy-Tera HPC Facility)

Figure 1.2: EUMETNET-SRNWP Overview of Operational Numerical Weather Prediction Systems in Europe as of October 2014. The complete model set-ups of the other NMS can be seen on *http://srnwp.met.hu*).

The use of GNSS for meteorological purposes was first proposed by *Bevis et al.* (1992). The capability of GNSS to produce continuous and high temporal resolution measurements appears has been shown to be beneficiary for the weather forecasts and particularly for improvement of the precipita-

tion prediction. With the availability of near real time and real time GNSS data it is now widely used in operational meteorology for model evaluation and assimilation. One of the applications of GNSS NRT data in NWP is for evaluation of the model skills in predicting water vapour dynamics. The GNSS ZTD dataset has high accuracy, with Root Mean Square (RMS) error around $3-4\,mm$, which corresponds to $0.4-0.6\,mm$ of IWV. There are two strategies for comparison of GNSS data sets and the NWP models. The fist of them is to calculate the IWV, using surface temperature and pressure from observation or model. The second strategy is to compare the ZTDs. For this comparison there is no need of using the surface temperature and pressure and the ZTDs are estimated directly from the model. For this study estimates of the IWV are compared.

There are many studies comparing the IWV from GNSS and NWP models in Europe. Four months GNSS and HIRLAM IWV comparison for Sweden and Finland (*Yang et al.*, 1999) gives an average offset of 0.1 mm, RMS difference 2.4 mm and correlation coefficient is 0.94. Another work with HIRLAM model analysis in Spain (*Cucurull et al.*, 2000) found IWV bias of 0.4 mm and RMS 2 mm. For sites ranging from Sweden to the Canary Islands *Vedel et al.* (2001) report a ZTD bias of 3.2 mm (17.1 mm standard deviation (SD)) between GNSS and HIRLAM analyses and short-term forecasts. *Haase et al.* (2003) found GNSS HIRLAM ZTD offsets for sites in western Europe, mainly near the Mediterranean, to be 3.4 mm ($\pm$ 18 mm SD). Both bias and SD decreased with altitude, bias was almost constant with latitude, while SD decreased with latitude. SD had a seasonal cycle, being largest in summer. In Estonia *Keernik et al.* (2014) found that HIRLAM underestimates the IWV by 59 % for values below 12 mm, and overestimates by 6-10 % for values over 25 mm. Comparisons between GNSS and COSMO IWV have been performed by the German Weather Service and the Swiss Federal Institute of Meteorology and Climatology. A study by *Kopken* (2001) reported a systematic, humid model bias of 2.53 mm over Sweden and Finland and a bias around 1mm over Germany. A study of the diurnal IWV cycle over Germany in summer 2000, found a systematic underestimation larger than 1 mm in the model analysis for the hours between 06 and 18 UTC (*Tomassini et al.*, 2002). In summer, the model has a significant dry bias during day-time of 1.03 mm. For Switzer-

land *Guerova et al.* (2003) report a good agreement between model analysis and GNSS in winter but in summer, a significant underestimation of IWV was found in the model which is well correlated with significant overestimation of light precipitation. For both Germany and Switzerland a systematic underestimation of the diurnal IWV cycle between 6 and 21 UTC in both the model analysis and forecast is reported in *Guerova and Tomassini* (September 2003). ZTD inter-comparison between the ALADIN model and GNSS (*Walpersdorf et al.* (2001)) show agreement on 6 mm level (corresponding to $\sim 1\,mm$IWV) for the North-west Mediterranean. The largest differences in ZTD ($> 20\,mm$), are found over limited periods of 1-3 days, mostly at coastal stations. Comparison of the ECMWF analyses to GNSS IWV (*Bock et al.* (2005)) at 21 stations in central Europe during the Mesoscale Alpine Programme experiment special observing period shows a dry model bias of about $1\,mm$ (5.5 %) $\pm$2.6 mm (13 %). The bias at individual sites varies from $-4\,mm$ to $0\,mm$. The largest differences are observed at stations located in mountainous areas and/or near the sea.

In the last 5 years GNSS meteorology is developed in Bulgaria as a part of a Marie Curie funded project. Studies of short and long term variation of IWV are presented in *Guerova et al.* (2014). In this study the GNSS IWV is derived using the surface temperature and pressure from NWP model. The derived GNSS IWV is used for evaluation of WRF model for 7 stations in Bulgaria. This is the first study of this type for the South-East Europe.

The thesis has four chapters. The first chapter is the introduction presenting the state-of-the-art. The second chapter describes the data sets used and gives information about processing and archiving in the Sofia University Atmospheric Data Archive (SUADA). The third chapter presents the results from inter-comparison of the IWV from GNSS and WRF. Yearly, monthly and diurnal analysis are presented. In chapter four the conclusions, outlooks and further work are presented.

Chapter 2

Data sets used

The main objective of the Global Navigational Satellite Systems (GNSS) is exact position determination. However, GNSS is used for a number scientific applications and one of which is atmospheric remote sounding. The advantage of the ground-based GNSS tropospheric products are continuous measurements not affected by rain or clouds. The GNSS technique provide tropospheric products with both high temporal and spatial resolution, suitable for operational weather forecasting and climate research. Because of these advantages of the ground-based GNSS tropospheric products are used as an independent source for evaluation of the NWP models.

2.1 GNSS tropospheric products for Bulgaria

2.1.1 GNSS processing

One of the GNSS networks in Bulgaria is operated the company BULiPOS (Bulgarian Intelligent Position determination System, *http://www.bulipos.eu/*). The BULiPOS network consists of 20 stations but in this work are used 7 stations marked with red pointers on figure 2.1. The network is mainly used for navigation and geodesy purposes, accuracy from a few meters to millimeters.

All raw GNSS data is provided from the BULiPOS network and was

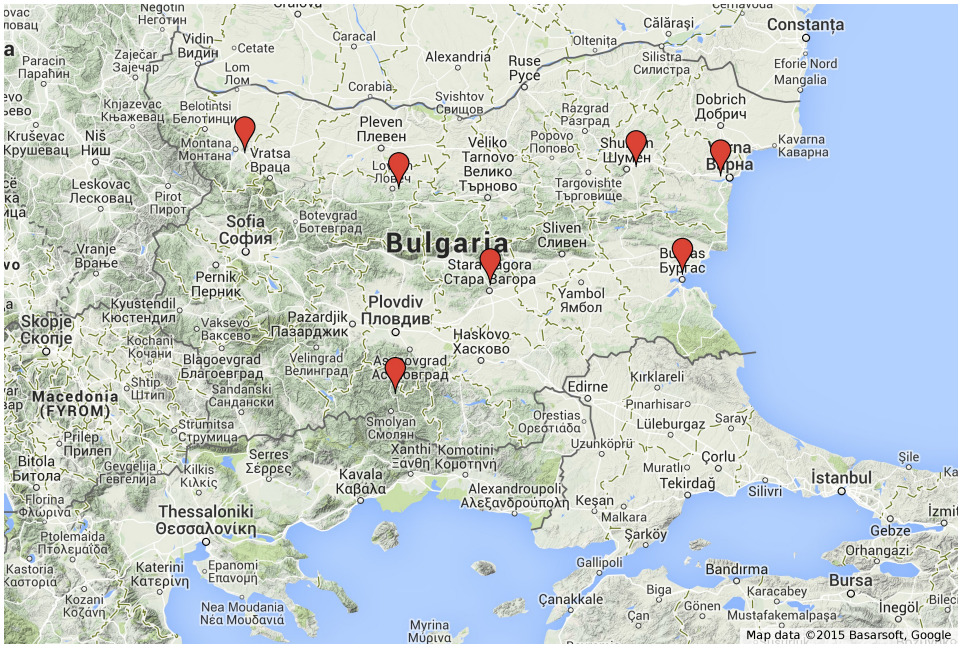

Figure 2.1: GNSS stations from the BULiPOS network in Bulgaria.

processed during the Short Term Scientific Mission (STSM) of Tzvetan Simeonov in 2014 to University of Luxembourg. Under the supervision of Prof. Norman Tefferle the GNSS tropospheric products (Zenith Total Delay, ZTD) were computed with the NAvigation Package for Earth Observation Satellites (NAPEOS, *http://www.positim.com/napeos.html*) software. NAPEOS is developed and maintained by the European Space Operations Centre (ESOC) of the European Space Agency (ESA). NAPEOS is used at ESOC since January 2008. The computed with NAPEOS tropospheric products are with temporal resolution 5 min for the 2013. The NAPEOS version 3.3.1 software (developed by ESA) was used for the processing of GNSS data. The processing was performed using GMF (Global Mapping Function) (*Boehm et al.*, 2006) and 10° elevation cut-off angle. The data was processed using Precise Point Positioning (PPP) strategy employing IGS (International GNSS Service) orbits and clocks for the satellites.

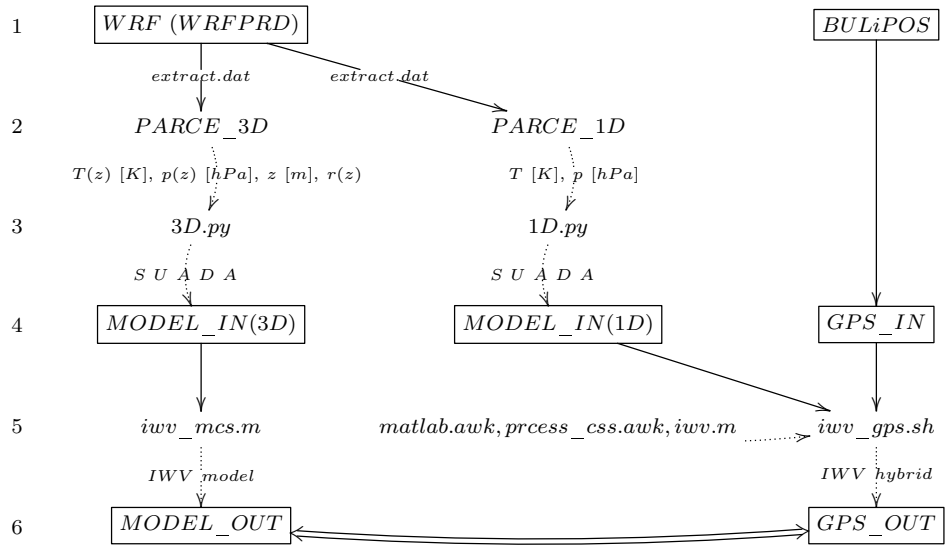

Figure 2.2: Data flow and archiving of GNSS and WRF IWV in SUADA.

2.1.2 Camputation of IWV hybrid

To derive IWV from GNSS the surface pressure $p[hPa]$ and temperature $T[K]$ from the WRF model are used. This type of IWV data is named "hybrid". In figure 2.2 the data flow of the archived in SUADA IWV hybrid data is presented. From the generated by the WRF model output file (extract.dat) and by using the PARCE_1D (Grid Analysis and Display System (GrADS), *http://iges.org/grads/*) and Python (*http://www.python.org*) scripts the surface pressure $p\,[hPa]$, temperature $T\,[K]$ and the terrain height $z_0\,[m]$ are extracted and uploaded in the MODEL_IN(1D) SUADA table. Using a MATLAB (*http://www.mathworks.com/*) routine the IWV hybrid is computed and saved in GPS_OUT table.

In order to derive IWV hybrid from GNSS first the Zenith Hydrostatic Delay (ZHD) is computed following *Elgered G.* (1991):

$$ZHD = (2.2768 \pm 0.0024)\frac{p_s}{f(\theta, h)} \tag{2.1}$$

where p_s is surface pressure and $f(\theta, h)$ is a factor, dependent on altitude h and the latitude variation of the gravitational acceleration θ:

$$f(\theta, h) = 1 - 0.00266cos(2\theta) - 0.00028h$$

The pressure at the GNSS station altitude is calculated using the model pressure at the nearest model grid point. The pressure difference between the GNSS station altitude and the nearest NWP model grid point is calculated using the polytropic barometric formula *Sissenwine N.* (1962):

$$P_g = P_m \left(\frac{T}{T - L(H_g - H_m)} \right)^{(\frac{g_0 M_0}{R * L})} \tag{2.2}$$

where P_g is the pressure at the GNSS station altitude, P_m is the pressure at meteorological station altitude, T is the temperature in meteorological station, $L = 6.5\ K/km$ is tropospheric lapse rate, H_m is the altitude of the meteorological station, H_g is the altitude of the GNSS station, $g_0 = 9.81\ m/s^2$ is the gravitational acceleration, $M_0 = 28.9\ g/mol$ is the molar mass of air and $R = 8.31432\ \frac{Nm}{(molK)}$ is the universal gas constant. The IWV is then calculated using:

$$IWV = \frac{10^6}{(\frac{k_3}{T_m} + k_2')R_v}\ (ZTD - ZHD) \tag{2.3}$$

where k_2', k_3 and R_v are constant and T_m is the weighted mean atmospheric temperature.

The surface pressure and temperature are key parameters in GNSS IWV derivation. As seen in figure 2.3 (*Guerova*, 2003) the surface pressure error of about 1 hPa will result in 0.35 mm IWV error, while 2 hPa will result in 0.7 mm and 3 hPa will be 1 mm IWV. The surface temperature has minor effect on the IWV estimations with 2 K error resulting in only 0.12 mm IWV error.

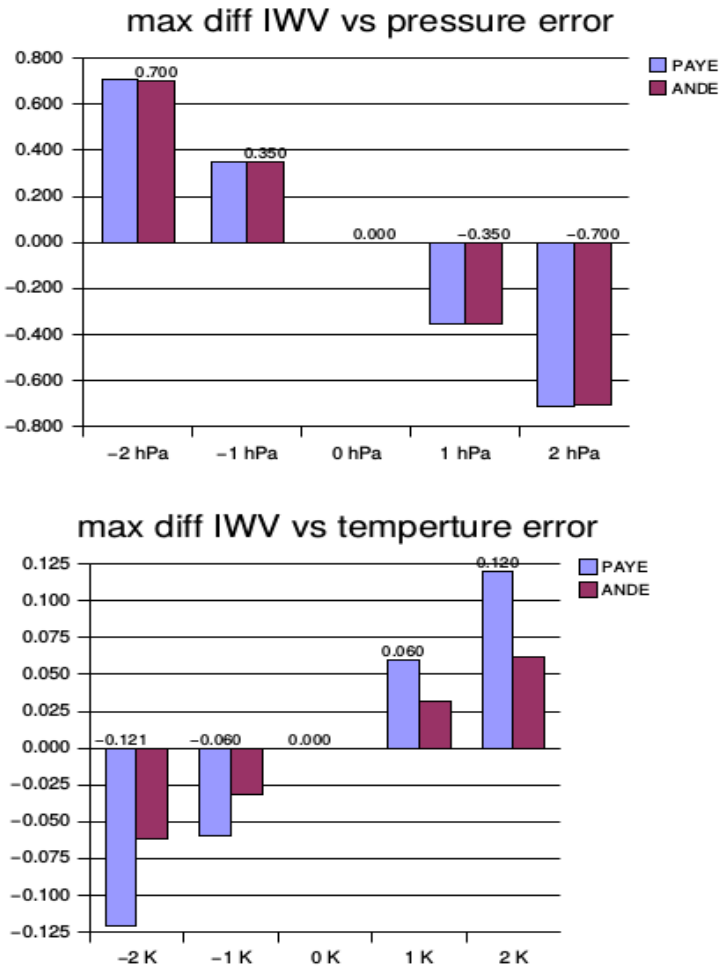

Figure 2.3: IWV error resulting from the surface pressure (top plot) and temperature (bottom plot) error.

2.2 Numerical Weather Research Model - WRF

In the last years the use of NWP models has been facilitated by increased power of supercomputers and achieving high spatial and temporal resolution is now possible ($\Delta x = 1.5\,km$). Improvements in the parametrizations schemes and representation of the atmospheric waves and convection was made. The need of reliable water vapour data is essential for improvement of the cloud parametrization schemes and to resolve boundary layer structures and dynamics.

2.2.1 WRF model set-up

The Weather Research and Forecasting (WRF) model is an atmospheric simulation system designed for both research and operational applications. It is developed by collaboration of National Center for Atmospheric Research's (NCAR) Mesoscale and Microscale Meteorology (MMM) Division, the National Oceanic and Atmospheric Administration's (NOAA), the National Centers for Environmental Prediction (NCEP) and Earth System Research Laboratory (ESRL), the Department of Defense's Air Force Weather Agency (AFWA) and Naval Research Laboratory (NRL), the Center for Analysis and Prediction of Storms (CAPS) at the University of Oklahoma, and the Federal Aviation Administration (FAA), with the participation of university scientists. The model is available from *http://www.wrf model.org*. The model version is 3.4.1, installed and operated on the University of Sofia Parallel Computer Center (Physon).

The WRF equations are Euler non-hydrostatic, the vertical component is terrain following and the horizontal grid is the Arakawa-C scheme. For the time integration the Runge-Kutta 2nd and 3rd order schemes are used. For initial and boundary conditions from the Global Forecasting System (GFS) model are used. No data is assimilated in WRF for this study. The WRF horizontal resolution is $9\,km$ and the vertical resolution is 44 levels, up to $20\,km$. The model domain is centred over Bulgaria and cover the South-East Europe (figure 2.4).

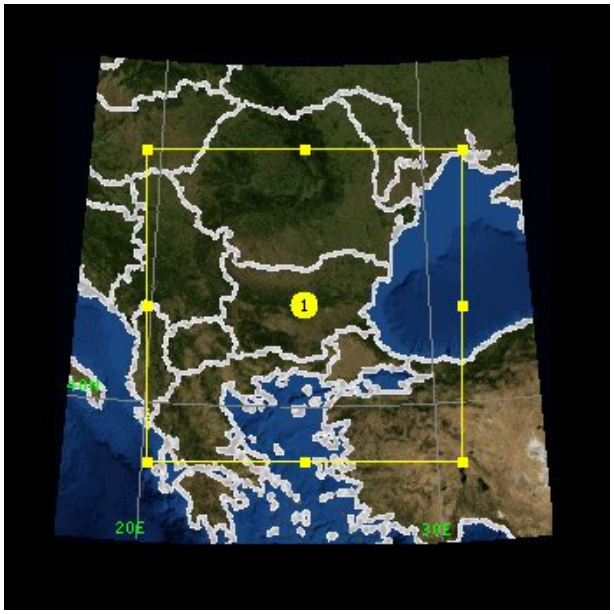

Figure 2.4: WRF model domain.

The parametrizations schemes for the model physics are:

- Unified Noah land-surface model for the land surface (LS)
- YSU scheme for the planetary boundary layer (PBL)
- WSM 6-class graupel scheme for the microphysics (MP)
- RRTM/RRTMG (Rapid Radiative Transfer Model) for the long-wave/ shortwave radiation.

2.2.2 Camputation of IWV model

Two type of WRF model fields are saved in SUADA database. The first are surface temperature $T\,[K]$, surface pressure $p\,[hPa]$ and the terrain height z_0 [m]. The second type of data are profiles of pressure $p(z)\,[hPa]$, temperature $T(z)\,[K]$, water vapour mixing ration $r(z)$ and the high of vertical level $z\,[m]$. In figure 2.2 the data flow of the archived in SUADA WRF and GPS IWV data is presented. The WRF model generates an output file "extract.dat" and

by using the GrADS PARCE_3D and Python scripts the vertical profiles of temperature, pressure and mixing ratio are uploaded in the MODEL_IN(3D) SUADA table. Using a MATLAB routine the IWV model is computed and saved in MODEL_OUT table. The IWV model is computed by first calculation of the water vapour density at each model level and then integration over model levels:

$$IWV = \frac{1}{\rho_w} \int_z^{z_n} \rho_{wv}(z)\, \mathrm{d}z \tag{2.4}$$

where ρ_w is density of liquid water, n is the number of model levels and $\rho_{wv}(z)$ is water vapour density.

2.3 Comparison of GNSS and WRF of stations' coordinates

The IWV field for 7 stations in Bulgaria for 2013 is compared. The IWV data is derived by using surface temperature and pressure from WRF model. The dataset, which uses GNSS data and WRF simulation for pressure and temperature is called Hybrid IWV. The temporal resolution of the model is 30 minutes but for this comparison 1 hour resolution is used. The data is presented in UTC (Coordinated Universal Time).

A comparison of GNSS stations' coordinates and WRF grid points from operational analyses is given in table 2.1 The GNSS estimates at each station are compared to the model output at the nearest grid point. The comparison is made between the GNSS and WRF datasets: Hybrid and Model. In the first column the names of the stations are given, in the second and third the altitude from the GNSS and WRF is given and in the forth the difference between GNSS and WRF altitudes. Four of the stations (Montana, Lovech, Stara Zagora and Varna) are situated below the WRF model grid point height and three stations (Burgas, Shumen and Rozhen) are above. Four of the stations have altitude difference less than 40 meters but for two stations Lovech and Rozhen it is respectively $-107.1\,m$ and $+348.0\,m$. These differences can lead to large biases in IWV values. In the last column the number of all available

days with data for each station are given.

Station name	GNSS altitude [m]	WRF altitude	GNSS-WRF [m]	Number of days with data
BURGAS	71.1	34.0	+37.1	306
VARNA	61.7	96.0	-34.3	253
LOVECH	243.0	350.1	-107.1	320
MONTANA	203.1	224.7	-21.7	289
SHUMEN	268.0	243.1	+24.9	308
STARA ZAGORA	227.1	254.2	-27.1	314
ROZHEN	1778.8	1430.8	+348.0	311

Table 2.1: GNSS (second column) and WRF (third column) altitude comparison, differences between the GNSS and WRF altitudes (forth column) and number of days with available data for every station (fifth column).

A comparison between Hybrid and Model data is presented for all stations. For sites Burgas, Varna and Lovech additional comparison with IWV estimates derived with surface temperature and pressure Observations is made. The dataset with NIMH pressure and temperature observations, combined with GNSS data from SUGAC is called Observed dataset. The Observation data for stations Burgas and Lovech is every 3 hours, while for the Hybrid and Model IWV, the temporal resolution is 1 hour.

Chapter 3

Evaluation of the WRF model IWV with GNSS-IWV for 2013

3.1 Evaluation of WRF model surface pressure and temperature

Before the analysis of IWV datasets, a comparison of surface pressure and surface temperature from WRF (red dots) and SYNOP observation (blue dots) is made. On figure 3.1 and figure 3.2 comparison for station Lovech is shown. The correlation coefficient for the pressure between the two data sets is 0.989 and the mean difference is 0.5 hPa. The correlation coefficient for the temperature is 0.957. In December the large differences in the two data sets are seen. For this comparison the data for every three hours is used. For station Varna the correlation coefficient for the pressure is 0.995 and for the temperature 0.960 with mean difference between the Observation and Model for the pressure 0.2 hPa and 0.2° C for the temperature. For station Burgas the correlation coefficient for the pressure is 0.995 and for the temperature 0.960. The mean difference between Observation and Model for the pressure is 0.1 hPa and 0.2° C for the temperature.

The evaluation of WRF surface pressure and temperature, presented in this section, shows very good overall agreement. This is important as in

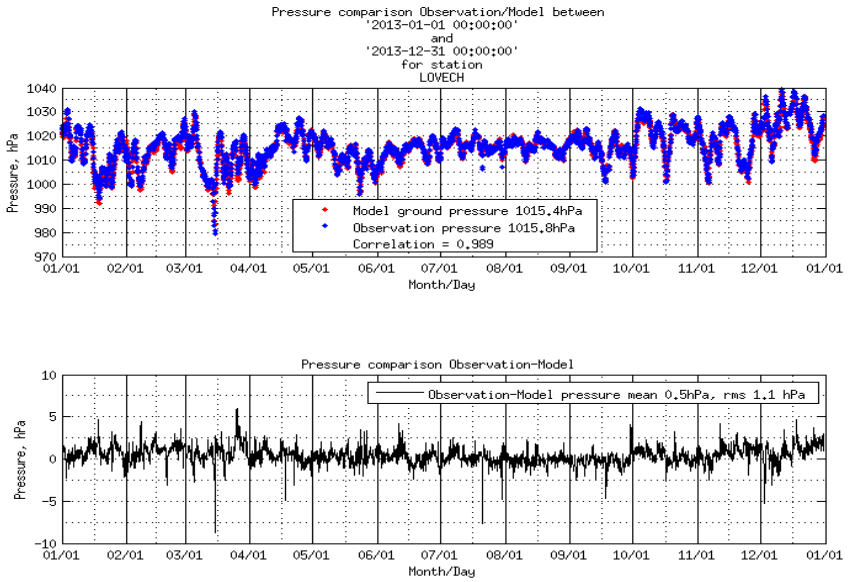

Figure 3.1: Observed (blue dots) and Modelled (red dots) pressure [hPa] for station Lovech in 2013 (top plot). Difference between Observed and Modelled pressure (bottom plot). Mean difference is 0.5 hPa and RMS 1.1 hPa.

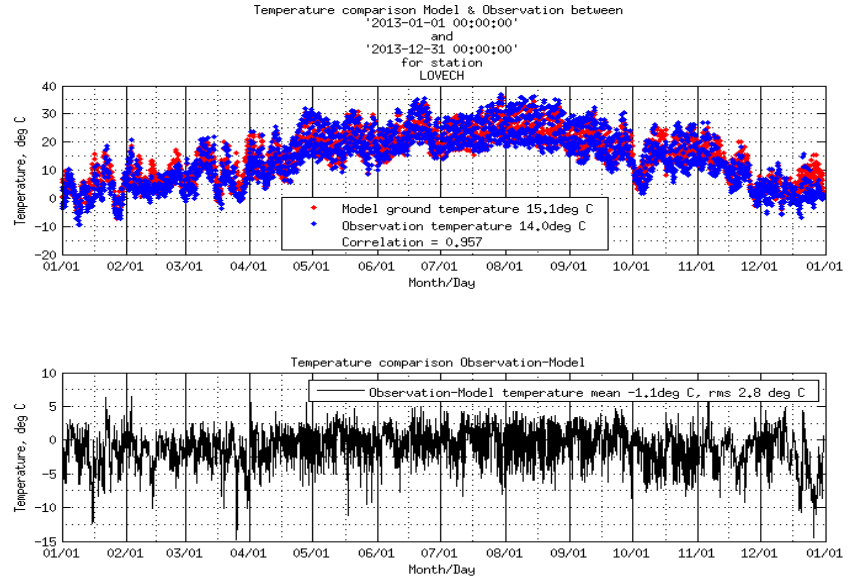

Figure 3.2: Observed (blue dots) and Modelled (red dots) temperature [° C] for station Lovech in 2013 (top plot). Difference between Observed and Modelled temperature (bottom plot). Mean difference 1.1° C and RMS 2.8° C.

order to take advantage of the high temporal resolution of GNSS tropospheric products (5 min), the model fields are used to derive GNSS IWV as described in section 2.1.

3.2 IWV diurnal cycle

In general the IWV from the Model shows good agreement with the Hybrid data. In all of the comparisons the diurnal cycle of the IWV derived with WRF model is well seen. The minimum values of the water vapour are around 5 UTC and maximum are around 15 UTC. The Observed dataset is available only for Lovech and Burgas. A detailed IWV comparison between the Model and Observed data also shows a very good agreement.

In the bottom plot of figure 3.3 is presented the diurnal cycle of IWV for station Burgas in 2013. A very good agreement between the IWV Observed (green line) and Hybrid (blue line) data points is present. The improved temporal resolution of the Hybrid IWV is clearly seen. The comparison of the Hybrid and Model (red line) IWV gives lower IWV in the Model. The mean difference between the two data sets is around 0.5 mm. The agreement is good in the morning hours but during the afternoon the difference becomes larger (around 1 mm, top plot). It can be noticed that there are two peaks in GNSS IWV at 13 UTC and 17 UTC, which are missing in the Model. In addition, the GNSS station altitude is 37 meters below the Model grid point.

The Observed and Hybrid IWV for station Lovech is shown in figure 3.4. There the comparison is also very good with only two points at 12 and 15 UTC with differences up to 0.5 mm. The difference in IWV between Hybrid and Model is 1.2 mm. It also can be noticed that the diurnal cycle has a smaller amplitude than in station Burgas. This can be attributed to the difference between the altitudes i.e. station Lovech is at 243 m asl. while Burgas is at 71 m asl.

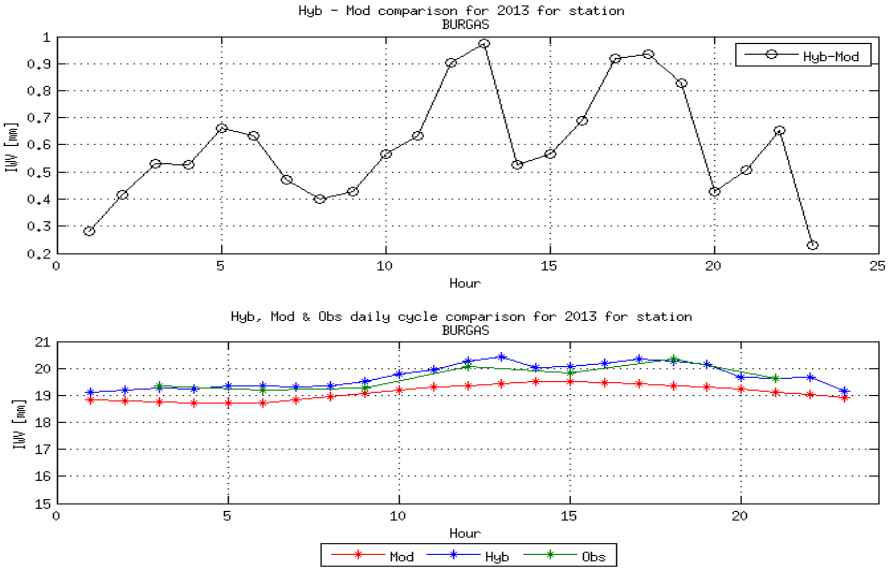

Figure 3.3: Top plot: difference between Hybrid and Modelled IWV. Bottom plot: diurnal cycle of Observed (green line with stars), Hybrid (blue line with stars) and Model (red line with stars) IWV for station Burgas in 2013.

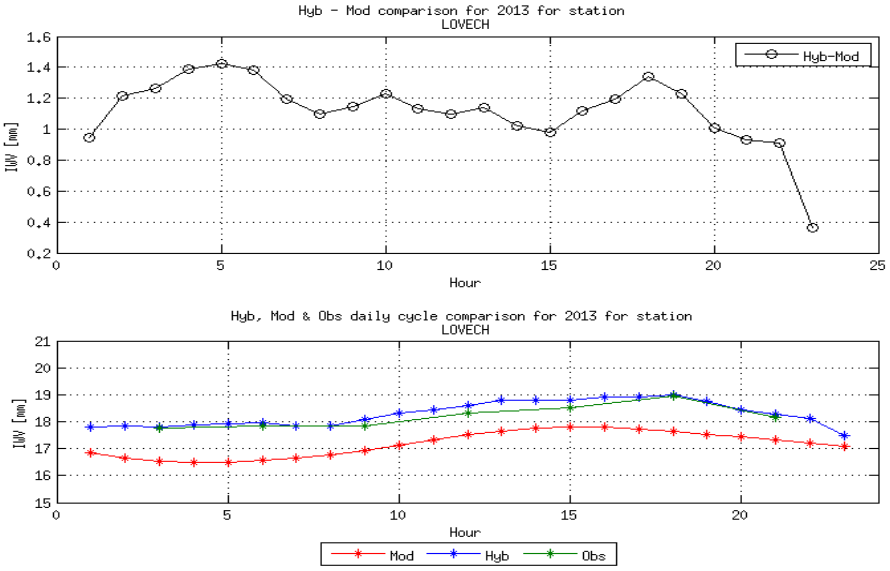

Figure 3.4: Top plot:difference between Hybrid and Modelled IWV. Bottom plot: diurnal cycle of Observed (green line with stars), Hybrid (blue line with stars) and Model (red line with stars) IWV for station Lovech in 2013.

For the next three stations only a Hybrid versus Model comparisons are made. For all of them the numerical analyses are showing a dry bias relative to the GNSS. For site Montana (figure 3.5) the estimated difference is $1.2\,mm$. Higher differences between datasets can be seen in the afternoon hours (top plot in figure 3.5).

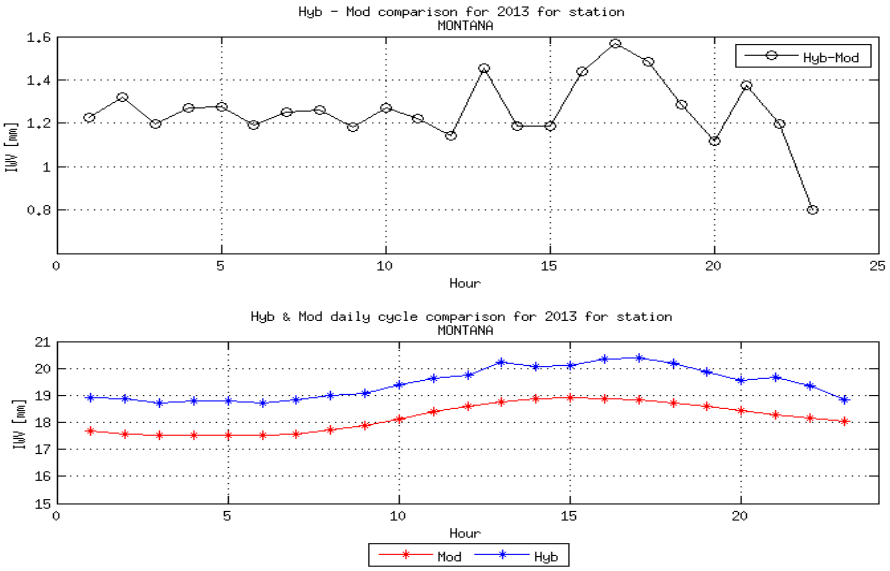

Figure 3.5: Top plot: difference between Hybrid and Modelled IWV. Bottom plot: diurnal cycle of Hybrid (blue line with stars) and Model (red line with stars) IWV for station Montana in 2013.

The diurnal variation of IWV in Montana is well presented as well as for station Shumen (figure 3.6) and Stara Zagora (figure 3.7). For both of them the mean difference is $0.5\,mm$. For site Shumen, which is in the northern part of Bulgaria the maximum of IWV is before 14 UTC while for Stara Zagora (southern Bulgaria) this peak is around 16 UTC.

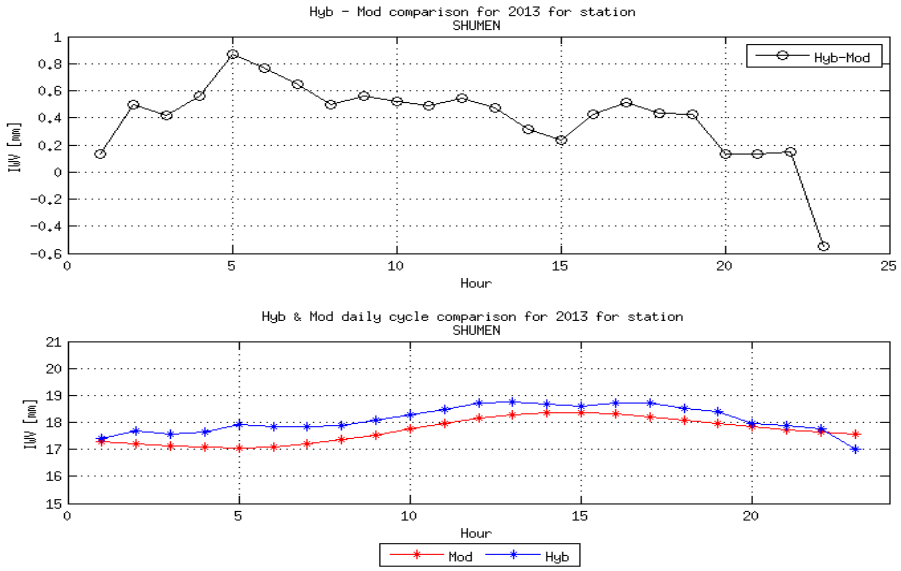

Figure 3.6: Top plot: difference between Hybrid and Modelled IWV. Bottom plot: diurnal cycle of Hybrid (blue line with stars) and Model (red line with stars) IWV for station Shumen in 2013.

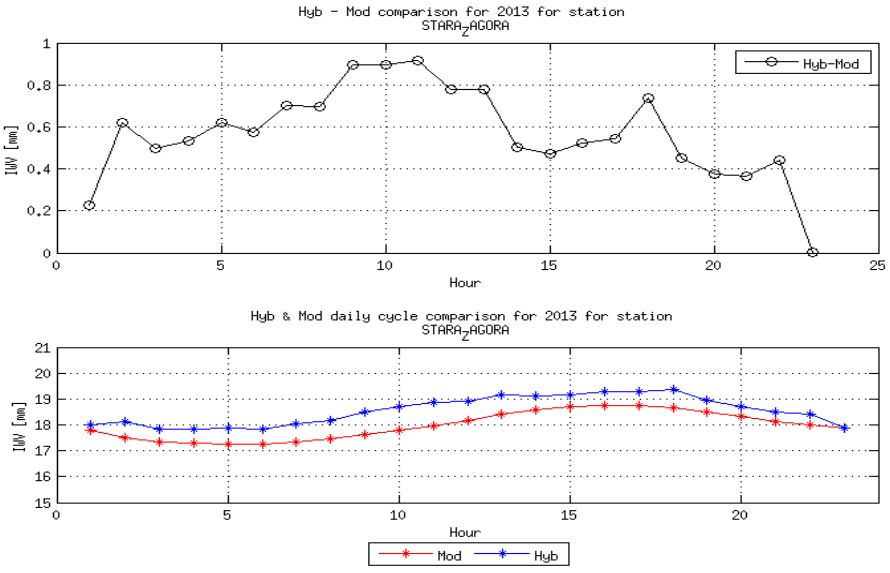

Figure 3.7: Top plot: difference between Hybrid and Modelled IWV. Bottom plot: diurnal cycle of Hybrid (blue line with stars) and Model (red line with stars) IWV for station Stara Zagora in 2013.

On figure 3.8 a IWV diurnal mean for stations Burgas, Shumen, Stara Zagora and Montana is presented. Stations Varna, Rozhen and Lovech are not included. The very high agreement in the diurnal variability is well presented for these stations with mean difference of 0.6 mm.

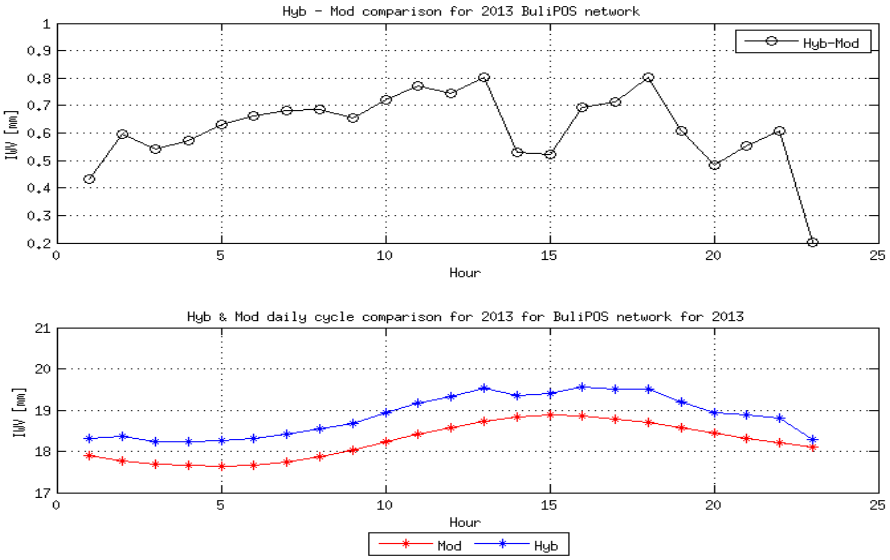

Figure 3.8: Top plot: difference between Hybrid and Modelled IWV. Bottom plot: diurnal cycle of Hybrid (blue line with stars) and Model (red line with stars) IWV for stations Burgas, Shumen, Stara Zagora and Montana in 2013.

3.3 IWV monthly comparison

In the figures 3.9 to 3.14 pictures are presented data for the comparison between the Hybrid and Model IWV with monthly mean values. The correlation coefficient for each month is also shown (top plots). The monthly mean IWV in June has a peak and is over 25 for all stations except Rozhen where the value is around 17 mm. These values are seen in the summer months. The minimum IWV amounts are during the winter months.

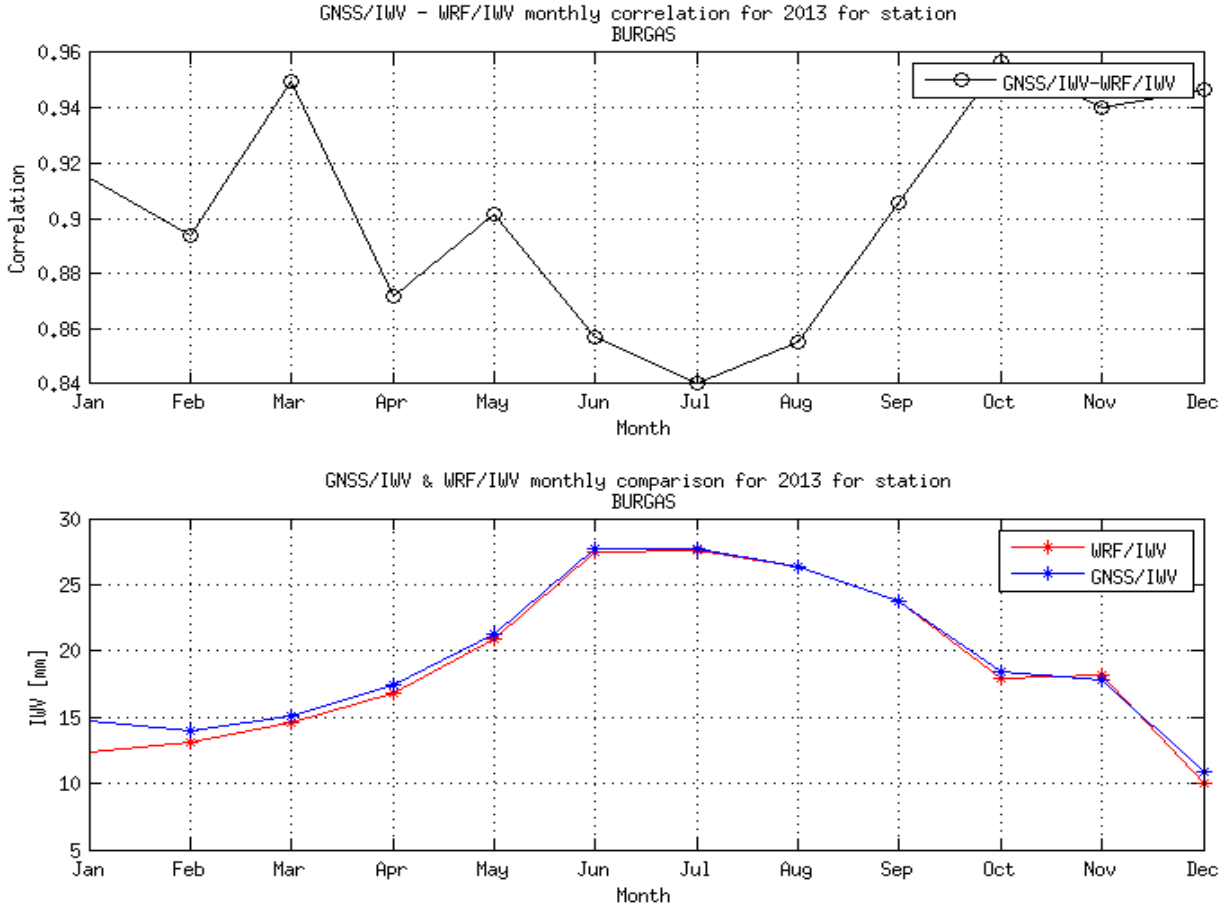

Figure 3.9: Monthly comparison between Hybrid and Model IWV (bottom plot) and correlation coefficient (top plot) for station Burgas in 2013.

The first comparison for station Burgas is shown in figure 3.9. It can be seen that there is good agreement between the Model and Hybrid for the annual cycle of IWV. The correlation coefficient is over 0.8. The maximum correlation is during the winter and autumn months and minimum in the sprint and summer. In particular interest is the jump between March, where the correlation is high and April where the correlation becomes smaller.

In figure 3.10 a comparison for station Lovech is presented. Here the highest correlation is in March 0.96 and lowest in April 0.84. Here a large change between March and April can also be seen. Station Lovech is situated in central North Bulgaria and station Montana (figure 3.11) is in Northwest

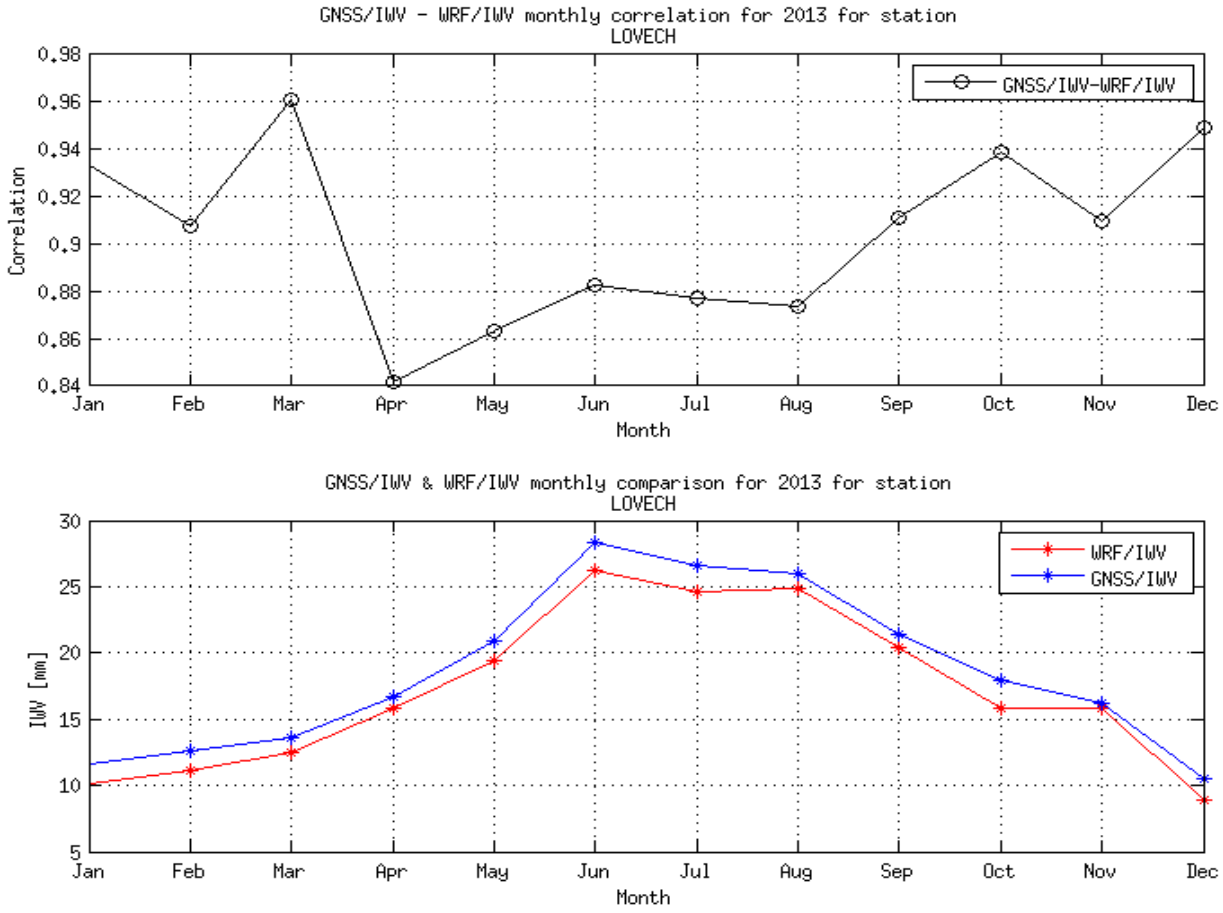

Figure 3.10: Monthly comparison between Hybrid and Model IWV (bottom plot) and correlation coefficient (top plot) for station Lovech in 2013.

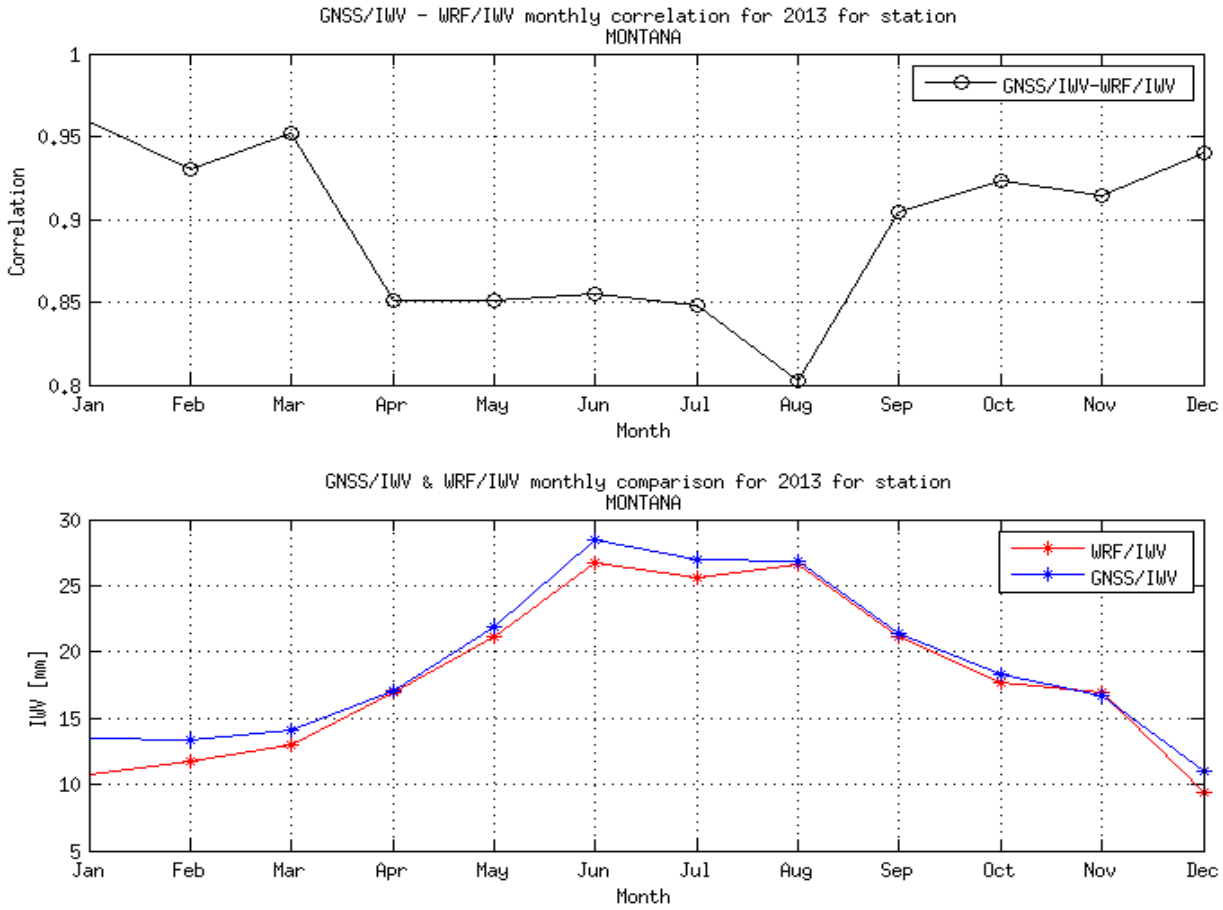

Figure 3.11: Monthly comparison between Hybrid and Model IWV (bottom plot) and correlation coefficient (top plot) for station Montana in 2013.

Bulgaria where the influence of the Balkan mountain is significant and the interaction with synoptic flows plays a major role for the IWV distribution. For these two stations the lowest Hybrid and Model IWV amounts are in December (around 12 mm) and highest is June (around 27 mm).

Between stations Shumen (figure 3.12) and Stara Zagora (figure 3.13) similarities in the IWV can be seen. The amounts are again maximum in June and minimum in December. For station Shumen the lowest correlation is in April and it stays low during the spring months. For station Stara Zagora the correlation coefficient stays low in with minimum from April till August.

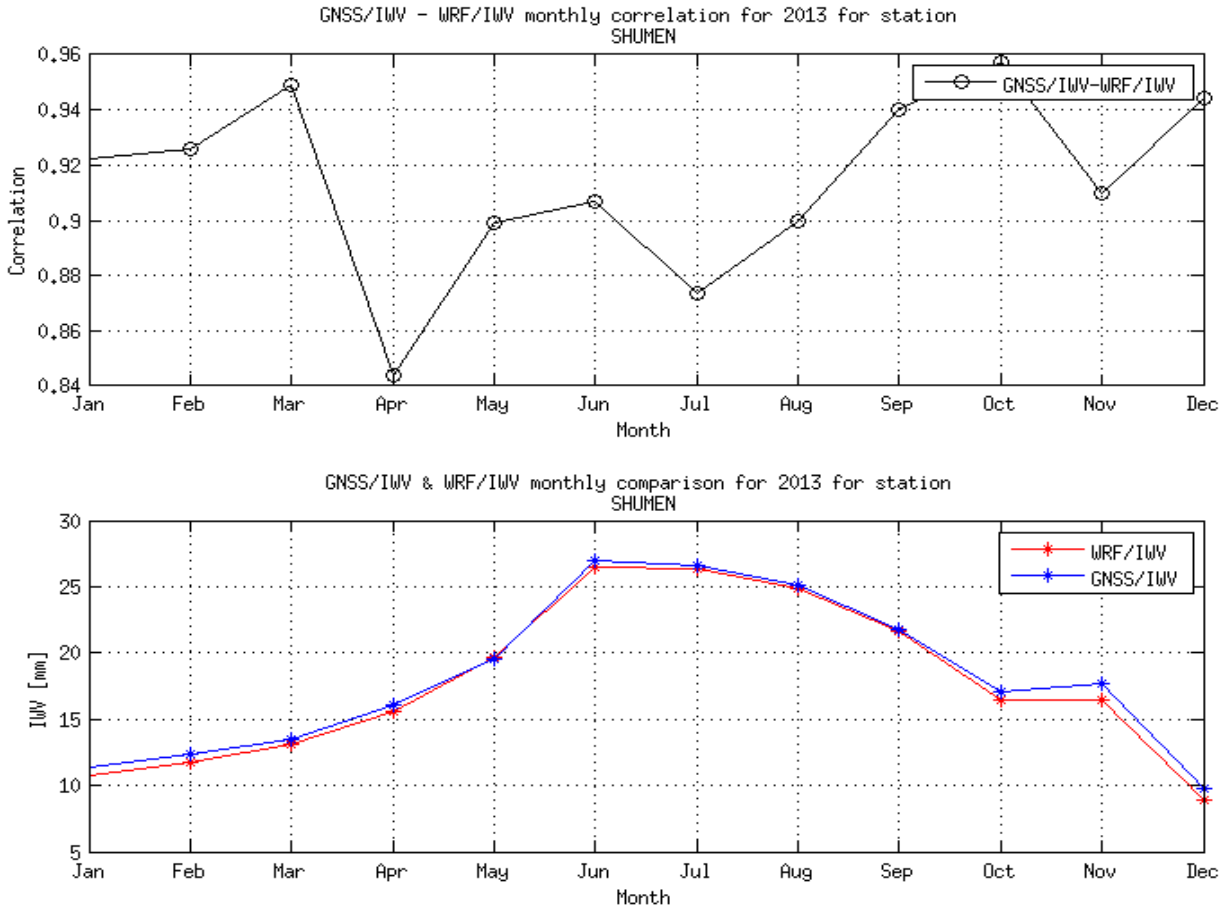

Figure 3.12: Monthly comparison between Hybrid and Model IWV (bottom plot) and correlation coefficient (top plot) for station Shumen in 2013.

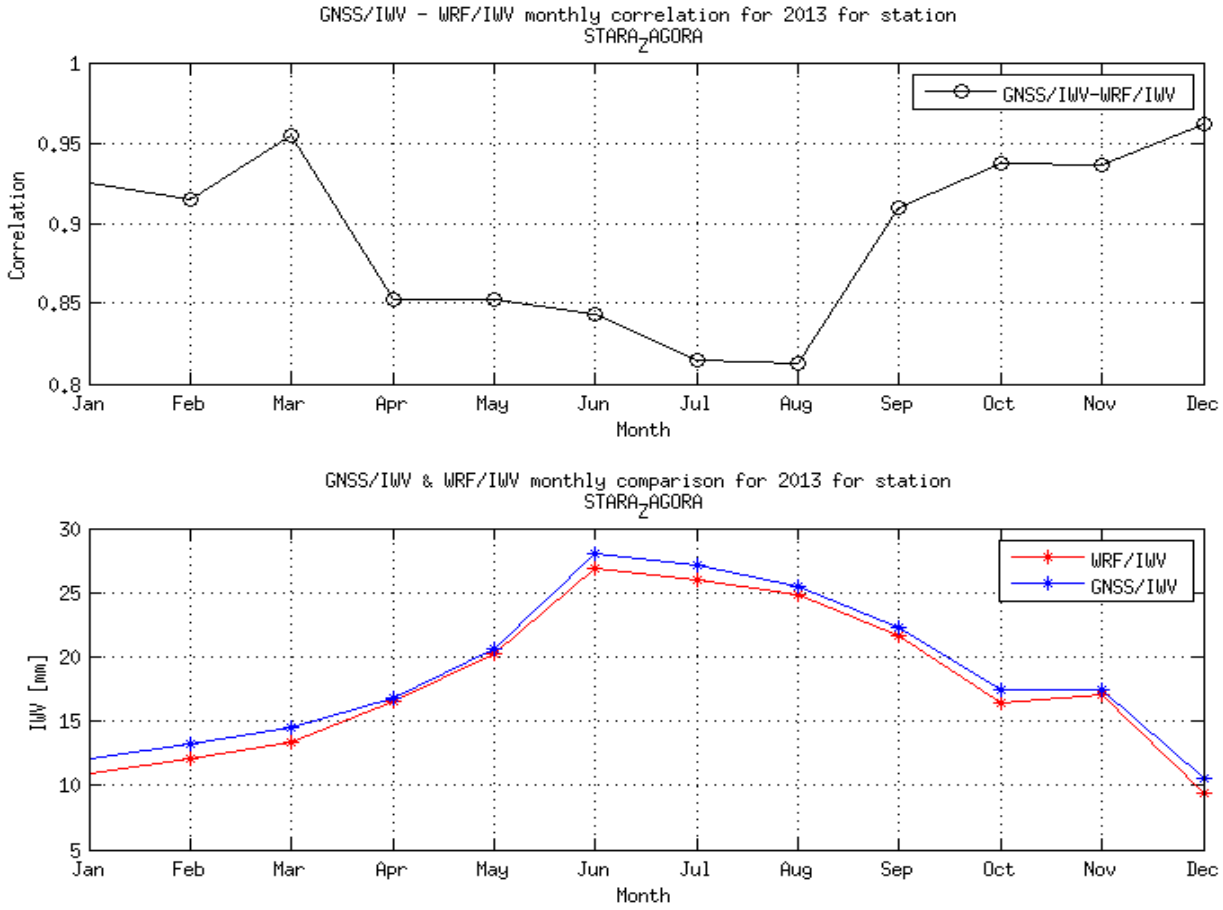

Figure 3.13: Monthly comparison between Hybrid and Model IWV (bottom plot) and correlation coefficient (top plot) for station Stara Zagora in 2013.

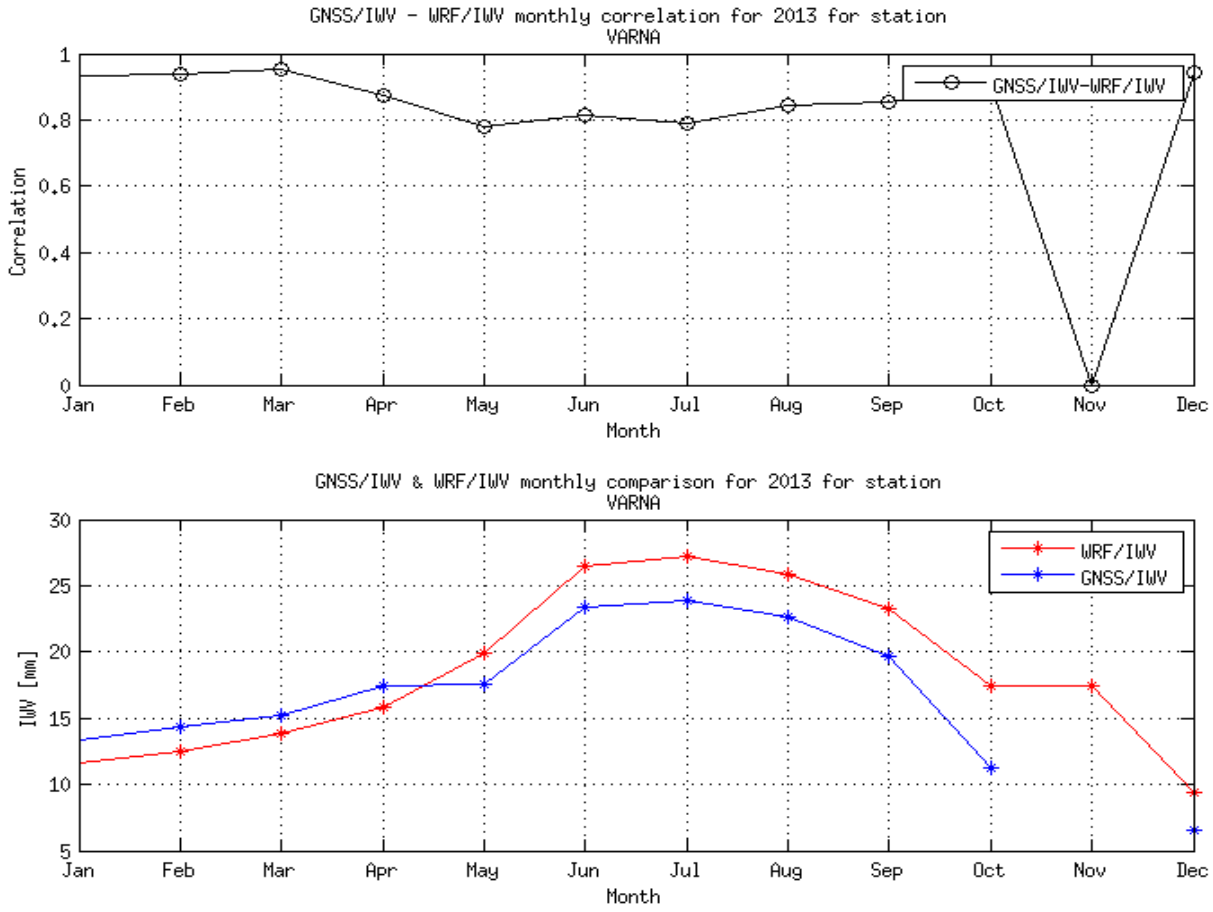

Figure 3.14: Monthly comparison between Hybrid and Model IWV (bottom plot) and correlation coefficient (top plot) for station Varna in 2013.

For station Varna (figure 3.14) of an interest is the difference between Hybrid and Model, which is seen during the months April and May. From January to April the IWV in the Model is lower than the Hybrid and from May to December it is the opposite. One of the possible reasons for this change is in the GNSS station set up, which will need further investigation.

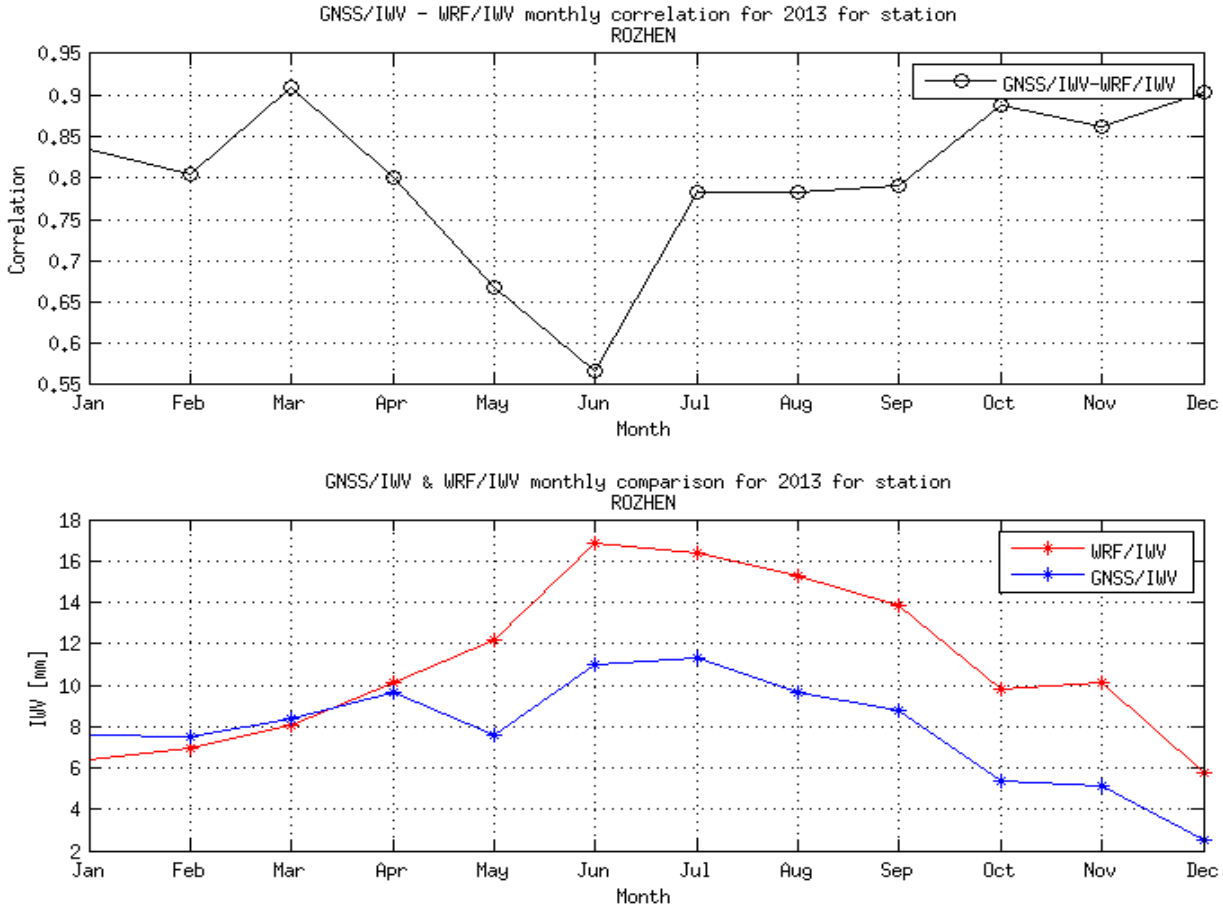

Figure 3.15: Monthly comparison between Hybrid and Model IWV (bottom plot) and correlation coefficient (top plot) for station Rozhen in 2013.

Station Rozhen (figure 3.15) is with worst representation for the IWV amounts for the monthly comparison and also for the diurnal cycle. Here the change in the Model IWV can be noticed. From January till April the Model shows lower IWV than Hybrid and from May onwards the opposite is seen.

3.4 IWV annual comparison

	Hybrid	Hybrid	Model	Model	Hybrid/Model	Hybrid-Model	Obs	Obs
Station	mean	SD	mean	SD	Correlation	Mean difference	mean	SD
MONT	19.4	7.6	18.0	7.4	0.953	1.4	-	
LOVE	18.2	7.6	16.5	7.2	0.963	1.7	17.0	7.3
SHUM	18.0	7.5	17.5	7.5	0.958	0.5	-	
BURG	19.6	7.5	19.1	7.7	0.957	0.5	19.4	7.6
STAR	18.5	7.5	17.3	7.4	0.959	1.2	-	
VARN	17.4	6.9	18.4	7.9	0.896	-1.0	17.3	7.0
ROZH	7.9	4.2	10.9	5.3	0.769	-3.0	-	

Table 3.1: Annual comparison with mean values and standard deviation (SD) for Model and Hybrid and mean difference between Hybrid and Model.

In Table 3.1 is presented comparison between the Hybrid and Model for the mean IWV values, their standard deviation (SD), mean difference and the correlation between the two methods. In the last two columns the Observation mean and SD for the three stations that are available are shown. The mean difference is worst for station Rozhen and for the rest of the sites is between $-1.0\,mm$ and $1.4\,mm$.

The scatter plots for six stations (Burgas, Varna, Lovech, Montana, Shumen and Stara Zagora) of the Model (X axis) and Hybrid (Y axis) IWV are presented on figure 3.16. For stations Burgas (top left) and Shumen (top right) smallest altitude difference can be seen, with data points equally spread along the best fit line. For the stations Stara Zagora (middle left) and Montana (middle right) an offset from the best fit line is observed, however the correlation coefficient still remains high (over 0.95). Here the greater part of the points can be seen over the best fit line. A large offset from the best fit line is seen for station Lovech (bottom left), however this can be explained with the to the high altitude difference between the Model and Hybrid. The altitude difference is for station Lovech is $107\,m$. For Varna station (bottom right) the spreaded outlier is largest and up to $20\,mm$ and the data sets are placed mostly above the best fit line and above $20\,mm$ are mostly bellow the best fit line.

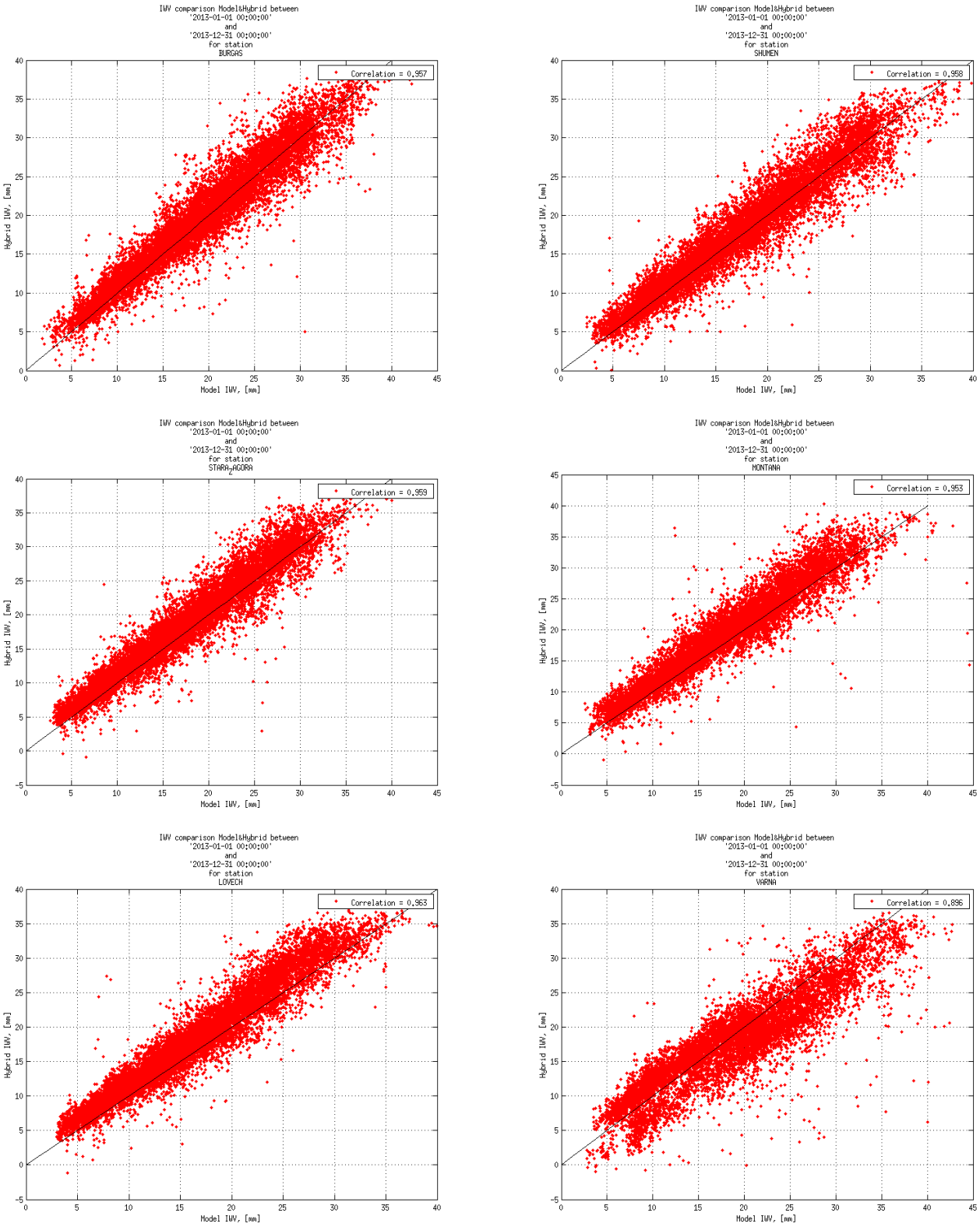

Figure 3.16: Annual IWV comparison between Hybrid and Model for station Burgas (top left), station Shumen (top right), station Stara Zagora (middle left), station Montana (middle right), station Lovech (bottom left) and station Varna (bottom right) in 2013.

Chapter 4

Conclusions

The WRF model and GNSS derived IWV across Bulgaria have been compared for 2013. Selected are seven stations in Bulgaria: Burgas, Varna, Lovech, Shumen, Stara Zagora, Montana and Rozhen. For station Lovech (also Burgas) surface temperature and pressure are compared from WRF model and observation. The correlation coefficient found to be 0.989 for the pressure and 0.957 for the temperature. The difference between Observation and Model pressure is 0.5 hPa and temperature -1.1 ° C. For two stations (Burgas and Lovech) comparison with Observation data for the IWV is made (stations Varna and Lovech are not presented here). The following conclusions can be made:

- The coordinates of the stations according to the Hybrid and Model are compared. It is observed that for the stations with higher altitude differences the representation of the IWV field is worse.
- The comparison for surface temperature and pressure derived by the Model and by the Observation show good agreement and correlation coefficient over 0.989.
- The results for the diurnal mean comparison showed that the diurnal cycle of IWV can be described well with largest differences between the Hybrid and the Model of water vapour up to 1.2 mm.

- The monthly mean comparison showed that during the summer months the correlation coefficient becomes smaller. During the winter months the IWV values are presented well with correlation coefficient over 0.900.
- The annual comparison showed mean difference between Hybrid and Model of the data sets between0.5 mm and 1.7 mm. Here the seasonal variation of the IWV can be seen well with maximum values in June and July.
- For station Rozhen and Varna there is a change between April and May of the monthly mean water vapour, which is likely due to changes of the station set-ups.

Appendix: Definition of statistics

For the calculation of the bias, mean, SD (standard deviation) and the correlation coefficient the following formulas are used:

$$bias = \frac{1}{N}\sum_{i=1}^{N}(IWV_{GNSS} - IWV_{WRF}) \tag{4.1}$$

$$\overline{GNSS_{IWV_{mean}}} = \frac{GNSS_{IWV_1} + ... + GNSS_{IWV_N}}{N} \tag{4.2}$$

$$SD_{GNSS} = \sqrt{\frac{1}{N}\sum_{i=1}^{N}(IWV_{GNSS} - \overline{IWV_{GNSS}})^2} \tag{4.3}$$

$$SD_{WRF} = \sqrt{\frac{1}{N}\sum_{i=1}^{N}(IWV_{WRF} - \overline{IWV_{WRF}})^2} \tag{4.4}$$

$$r_{(GNSS,WRF)} = \frac{\sum_{i=1}^{N}(IWV_{GNSS_i} - \overline{IWV_{GNSS}})(IWV_{WRF_i} - \overline{IWV_{WRF}})}{\sqrt{\sum_{i=1}^{N}(IWV_{GNSS} - \overline{IWV_{WRF}})^2 \sum_{i=1}^{N}(IWV_{WRF_i} - \overline{IWV_{WRF}})^2}} \tag{4.5}$$

Acknowledgments

I would like to thank:

- Assoc. Prof. G. Guerova for helping and encouraging me during my study
- Tzvetan Simeonov for his help with operating the SUADA and GNSS processing.
- Dr. Stoyan Pisov for the technical support with WRF model runs and postprocessing.
- Assoc. Prof. Elisaveta Peneva for helping me with the GrADS system
- Prof. Norman Teferle from University of Luxembourg for helping our team with the GNSS data processing campaign
- The BULiPOS company for the providing the GNSS data.

Bibliography

Bevis, M., S. Businger, T. A. Herring, C. Rocken, R. A. Anthes, and R. H. Ware, Gps meteorology: Remote sensing of atmospheric water vapour using the global positioning system, *J. Geophys. Res.*, *97*(14), 15,787–15,801, 1992.

Bock, O., C. Keil, E. Richard, C. Flamant, and M.-N. Bouin, Validation of precipitable water from ecmwf model analyses with gps and radiosonde data during the map sop, *Q. J. R. Meteorol. Soc.*, *131*, 3013–3036, doi: 10.1256/qj.05.27, 2005.

Boehm, J., A. Niell, P. Tregoning, and H. Schuh, Global mapping function (gmf): A new empirical mapping function based on numerical weather model data, *Geophysical Research Letters*, *vol.33, issue 7*, dOI: 10.1029/2005GL025546, 2006.

Cucurull, L., B. Navascues, G. Ruffini, P. Elosegui, A. Rius, and J. Vila, The use of gps to validate nwp systems: the hirlam model., *Journal of Atmospheric and Oceanic Technology*, *17*(6), 773–787, 2000.

Elgered G., e., Geodesy by radio interferometry water vapor radiometry for estimation of the wet delay, *Journal of Geophysical Research*, *96*, 6541–6555, 1991.

Guerova, G., Using gps data to validate mesoscale weather forecast model, Presentation at Institute of Applied Physics, University of Bern, 2003.

Guerova, G., and M. Tomassini, Monitoring iwv from gps and limited - area forecast model, *Tech. Rep. 2003-15*, University of Bern, Switzerland, September 2003.

Guerova, G., E. Brockmann, J. Quiby, F. Schubiger, and C. Matzler, Validation of nwp mesoscale models with swiss gps network agnes, *Journal of Applied Meteorology*, *42*, 141–150, 2003.

Guerova, G., T. Simeonov, and N. Yordanova, The sofia university atmospheric data archive (suada), *Atmospheric Measurement Techniques*, *7*(8), 2683–2694, doi:10.5194/amt-7-2683-2014, 2014.

Haase, J., M. Ge, H. Vedel, and E. Calais, Accuracy and variability of gps tropospheric delay measurements of water vapor the western mediterranean, *Journal of Applied Meteorology*, *42*, 1547–1568, 2003.

http://iges.org/grads/, Grid analysis and display system (grads).

http://srnwp.met.hu, Project: Coordination on short-range numerical weather prediction programme (c-srnwp).

http://www.bulipos.eu/, Gps and glonass satellite system bulipos.

http://www.egvap.dmi.dk/, The eumetnet eig gnss water vapour programme.

http://www.glonass.it/eng/, Global navigational satellite system.

http://www.gsa.europa.eu/galileo/services, European global navigation satellite systems agency.

http://www.mathworks.com/, Matlab language.

http://www.noaa.gov/, National oceanic and atmospheric administration.

http://www.positim.com/napeos.html, Napeos software for processing gnss data.

http://www.python.org, Python programming language.

http://www.wrf model.org, Weather and research forecasting model.

http://www.www.oso.chalmers.se/users/kge/cost716.html/, Cost action 716.

Keernik, H., H. Ohvrila, E. Jakobsona, Rannata, and A. Luhamaaa, Column water vapour: an intertechnique comparison of estimation methods in estonia, *Proceedings of the Estonian Academy of Sciences*, *63*(1), 37–47, 2014.

Kopken, C., Validation of integrated water vapor from numerical models using ground-based gps, ssm/i, and water vapor radiometer measurements, *Journal of Applied Meteorology*, *40*(6), 1105–1117, 2001.

Sissenwine N., e., The u.s. standard atmosphere, *Journal of Geophysical Research*, *67*, 3627–3630, 1962.

Tomassini, M., G. Gendt, G. Dick, M. Ramatschi, and C. Schraff, Monitoring of integrated water vapor from ground-based gps observations and their assimilation in a limited-area model, *Phys. and Chem. of the Earth*, *27*, 341–346, 2002.

Vedel, H., K. S. Mogensen, and X.-Y. Huang, Calculation of zenith delays from meteorological data comparison of nwp model, radiosonde and gps delays., *Physics and Chemistry of the Earth, Part A: Solid Earth and Geodesy*, *26*(6), 497–502, 2001.

Walpersdorf, A., E. Calais, J. Haase, L. Eymard, M. Desbois, and H. Vedel, Atmospheric gradients estimated by gps compared to a high resolution numerical weather prediction (nwp) model, *Physics and Chemistry of the Earth, Part A*, *26*(3), 147–152, 2001.

Yang, H., B. H. Sass, G. Elgered, J. M. Johansson, and T. R. Emardson, A comparison of precipitable water vapor estimates by an nwp simulation and gps observations., *Journal of Applied Meteorology*, *38*(7), 941–956, 1999.